Nuclear Instruments and Methods in Physics Research A302 (1991) 69–75
North-Holland

A study on radiation damage in doped BGO crystals *

R.Y. Zhu, H. Stone [1] and H. Newman
California Institute of Technology, Pasadena, CA 91125, USA

T.Q. Zhou, H.R. Tan and C.F. He
Shanghai Institute of Ceramics, Academia Sinica, People's Republic of China

Received 30 May 1990 and in revised form 21 September 1990

We report on a study of the correlation between radiation damage of bismuth germanate (BGO) scintillator crystals and trace impurities in the crystal. The light yield and the absorption spectra of doped BGO crystals were measured, both before and after irradiation. While trace concentrations of Cr, Mn, Fe and Pb in BGO were found to lead to substantial radiation damage, traces of Al, Ca, Cu and Si were found to have no measurable effect. Traces of Co, Ga, Mg and Ni were found to have an effect intermediate between the above two groups. Three radiation-induced absorption bands were observed in a set of BGO crystal samples. Their energy levels were found to be independent of the trace elements in the BGO. They are at 2.3 ± 0.1, 3.0 ± 0.1 and 3.8 ± 0.1 eV, respectively, above the valence band. A brief discussion of the radiation damage mechanism in BGO is presented.

1. Introduction

In the past fifteen years, bismuth germanate ($Bi_4Ge_3O_{12}$, commonly known as BGO) [1] has come to be recognized as a crystal scintillator whose short radiation length (1.12 cm), relatively high light output and short decay time (300 ns) make it attractive for a wide range of applications. It is currently used in pure and applied research in the fields of geological exploration, medicine, nuclear physics and high-energy physics. In high-energy physics, a large quantity of BGO crystals has been produced to build high resolution electromagnetic calorimeters. One example is the L3 electromagnetic calorimeter which consists of 11 000 large (150 cm^3 and 1.1 kg) BGO crystals [2]. The performance of the L3 BGO calorimeter shows that one can achieve an energy resolution of better than 1% above a few GeV.

BGO is known to suffer radiation damage, which has restricted its usage in some applications. Early work by Kobayashi et al. [3] shows that BGO's radiation susceptibility is related to the total concentration of impurities in the crystal. However, correlations between radiation damage and the chemical nature of the impurity in the crystal were not studied.

In the process of building the L3 BGO electromagnetic calorimeter, the radiation damage problem was studied systematically, through a collaboration between Caltech and the Shanghai Institute of Ceramics (SIC). A set of BGO crystals, doped with various elements was produced by the SIC, and was tested at Caltech.

In this report, we present data showing the correlation between radiation damage and the specific trace elements in a BGO crystal. While the trace impurities of Cr, Mn, Fe and Pb in BGO were found to result in substantial radiation damage, the presence of traces of Al, Ca, Cu and Si in BGO were found to have no measurable effect. Traces of Co, Ga, Mg and Ni in BGO were found to have an effect intermediate between the above two groups. This work thus has had a practical application in establishing a series of specifications on the maximum trace element concentrations allowed in the raw materials used to produce high-quality BGO crystals. In doing so, only the most harmful elements are specified, rather than to attempt a costly process of overall purification.

The radiation-induced absorption band spectrum in BGO also was studied, in order to learn about the nature of the radiation damage mechanism. Three radiation-induced absorption bands were found, common to all BGO samples, at 2.3 ± 0.1, 3.0 ± 0.1 and 3.8 ± 0.1 eV, above the valence band. This result indicates that the color centers in BGO crystals are related to the bulk elements in the BGO, and are not related to a specific impurity. Because the intensity of each band is indeed a function of the impurity type and its concentration, impurities in BGO appear to act as "catalytic agents" which activate pre-existing color centers in the BGO.

* Work supported in part by U.S. Department of Energy contract no. DE-AC03-81-ER40050.

[1] Present address: Physics Department, Geneva University, Geneva, Switzerland.

0168-9002/91/$03.50

Section 2 of this report describes the sample preparation and the experimental instrumentation used. Section 3 presents the results of our measurements and a brief discussion of the radiation damage mechanism in BGO. Our conclusions are presented in section 4.

2. Sample preparation and experimental methods

2.1. Sample preparation

The Bridgeman–Stockbarger method was used to grow a series of BGO crystals. Powders of 5N Bi_2O_3 and 6N GeO_2 were mixed in a stoichiometric ratio of 2:3 to provide the melt. A large BGO crystal was grown from the melt, and was powdered again to provide a new melt, which was used to grow a new crystal. This process was repeated three times, and the pure crystal produced was then powdered again to provide the melt for the doped BGO crystals used in our tests.

A certain amount of dopant was introduced into the melt, in the form of an oxide, during the final growth-cycle (as described above), to produce each doped crystal. A typical dopant concentration was 0.2 mmol/(kg BGO). Some dopants (Pb and Fe) were introduced at different levels, in different crystals, in order to study their effect quantitatively. In addition, slightly nonstoichiometric crystals were grown by adding extra Bi_2O_3 or GeO_2 to the melt in order to study the nature of the color centers.

In this report, crystals are identified by the chemical symbol of the dopant element. Where more than one level of dopant concentration was introduced, the different samples are distinguished by a number in brackets after the chemical symbol. The undoped samples are named L(1), L(3) and HS. L(1) is a sample cut from a large crystal which was grown only once. Sample L(3) is a sample cut from the "three times grown" crystal, which was powdered to provide the melt for all doped samples. Sample HS is a crystal cut from a ∅ 1 in. cylindrical sample provided by the Harshaw Chemical Co.

All samples were roughly $1 \times 1 \times 3$ cm^3 in size. Table 1 lists their weight and the dopant concentration introduced in the melt. No macroscopic imperfections, such as veils, voids, or large inclusions were visible.

The presence of trace elements in samples was analyzed by using the neutron activation method at the U.C. Irvine reactor facility [4]. The results of this analysis are presented in table 2. It is clear that, with the exception of Cu and Al, the dopant elements are present at levels much higher than those that might result from contamination during the manufacturing process. The exceptions, Cu and Al, are most likely introduced at the crystal manufacturing stage, and not as impurities in the raw materials. Aluminum oxide, for example, is used in the construction of the ovens. We note that crystal L(1) has the highest concentration of aluminum and crystal Ca has the highest concentration of Cu. The crystal from Harshaw also has a measurable Al contamination.

Table 1
The samples: dopant concentration in melt

Sample	Weight [g]	Dopant concentration in melt [ppm]
L(1)	20.9	–
L(3)	13.8	–
HS	27.8	Harshaw
Bi(1)	21.0	418.0
Bi(2)	21.0	4200.0
Ge(1)	21.1	145.0
Ge(2)	21.5	1451.0
Al	21.0	5.4
Ca	15.0	8.4
Cu	21.2	12 7
Si	21.0	5 3
Co	21.3	11 8
Ga	20.5	13 2
Mg	21.1	5 1
Ni	20 7	11 7
Cr	20.7	10.4
Mn	20 9	11.0
Fe(1)	17.4	5 6
Fe(2)	17 4	11.2
Fe(3)	16.2	16.7
Fe(4)	16.7	22.3
Pb(1)	20.4	20.7
Pb(2)	21.1	41.4
Pb(3)	20.9	62.2
Pb(4)	20 8	82.9

2.2. Irradiation source

All the irradiations were performed with a ^{137}Cs γ-ray source located in the Geology Department at CALTECH. The doses were delivered over a period of several hours, at a rate of 22.3 Gy/h.

2.3. Light output measurement

The scintillation light yield of BGO samples irradiated with a ^{137}Cs γ-ray source was measured by using a Hamamatsu photomultiplier tube (PMT) R1306. The spectral response of this PMT fits well the emission spectrum of the BGO. The scintillation light collected with Hamamatsu R1306 was integrated and digitized by a home-made QVT (integrated charge, peak voltage and time measuring device) in the Q (charge) mode. The digital signal from the QVT was sent to a Z80 microprocessor. The spectrum obtained was analyzed in the Z80. The peak ADC values were then obtained by a simple Gaussian fit.

The crystals were air-coupled to the PMT. The distance of the crystals to the PMT was regulated by a guide attached to the tube, so that the systematic error introduced in the pulse height, when the crystal was repeatedly removed from the tube and then re-attached to the tube, was found to be less than 0.5%.

All the measurements were done at the room temperature. The pulse heights were corrected for the temperature variation in BGO light output of $-1.6\%/°C$. The systematic error due to temperature uncertainties was estimated to be less than 0.25%.

2.4. Absorption spectrum measurement

A Hewlett Packard HP8450 Diode Array UV/VIS Spectrophotometer was used to measure the absorption spectra for each of the BGO samples. This spectrophotometer has a wavelength coverage of 250 to 800 nm. Corrections for the spectral response of the photodiodes in the spectrophotometer, for the spectral intensities of the light sources and for the absorption by the atmosphere were made automatically by the spectrophotometer. The wavelength scale was calibrated with a holmium oxide standard. The wavelength resolution of the instrument was found to be 1 nm for wavelengths below 400 nm, and 2 nm for wavelengths above 400 nm. The data obtained with this photospectrometer were transferred to a VAX 11/780 computer, and were analyzed on that computer.

The absorption spectrum of the Cr doped sample in the near infrared range was also investigated with a CARY 17 spectrophotometer. The infrared absorption spectra were taken with a Nicolet Instruments Fourier transform spectrophotometer.

3. Results

3.1. Light yield measurement

Before irradiation all crystals were clear, transparent and colorless. The only exception was the BGO crystal doped with Cr, which looked yellowish. The pulse heights measured with a ^{137}Cs source before irradiation are listed in the first column of the table 3. The data show that the light yield of all doped samples is comparable to that of the undoped samples, except the crystal doped with Cr. The light output of the crystal with Mn is also reduced (by a lesser, but significant amount). As reported below, the reduced light output in these two exceptional cases is associated with perma-

Table 2
Neutron activation analysis results

Sample	Trace concentration					
	Al [ppm]	Mn [ppm]	Cr [ppm]	Co [ppb]	Fe [ppm]	Cu [ppm]
L(1)	2.29 ± 0.04	< 0.039	< 0.029	< 0.30	< 0.07	0.95 ± 0.28
L(3)	0.16 ± 0.02	< 0.043	< 0.051	< 0.70	< 0.21	1.12 ± 0.32
HS	0.20 ± 0.02	< 0.040	< 0.032	< 0.40	< 0.12	< 0.69
Bi(1)	0.13 ± 0.01	< 0.036	< 0.048	< 0.50	< 0.14	< 0.52
Bi(2)	1.08 ± 0.03	< 0.034	< 0.044	< 0.50	< 0.14	0.70 ± 0.26
Ge(1)	0.05 ± 0.01	< 0.034	< 0.044	0.5 ± 0.2	< 0.13	0.73 ± 0.25
Ge(2)	1.03 ± 0.03	< 0.033	< 0.044	0.5 ± 0.2	< 0.13	0.93 ± 0.26
Al	0.30 ± 0.02	< 0.031	< 0.052	< 0.50	< 0.13	0.81 ± 0.26
Ca	0.05 ± 0.01	< 0.040	< 0.067	< 0.60	< 0.21	1.17 ± 0.32
Cu	0.39 ± 0.02	< 0.033	< 0.043	< 0.50	< 0.17	< 0.52
Si	0.85 ± 0.03	< 0.036	< 0.052	0.5 ± 0.2	< 0.13	< 0.52
Co	0.82 ± 0.03	< 0.033	< 0.050	63.7 ± 0.9	< 0.27	< 0.52
Ga	0.04 ± 0.01	< 0.035	< 0.052	< 0.50	< 0.13	0.52 ± 0.26
Mg	0.13 ± 0.01	< 0.036	< 0.052	< 0.50	< 0.13	< 0.52
Ni	0.09 ± 0.01	< 0.034	< 0.060	0.7 ± 0.2	< 0.15	< 0.51
Cr	0.14 ± 0.01	< 0.034	0.219 ± 0.030	< 0.50	< 0.15	< 0.52
Mn	0.05 ± 0.01	0.241 ± 0.026	< 0.032	< 0.30	< 0.13	0.91 ± 0.25
Fe(1)	0.10 ± 0.01	< 0.038	< 0.037	0.8 ± 0.2	0.13 ± 0.04	0.93 ± 0.29
Fe(2)	0.07 ± 0.01	< 0.041	< 0.038	< 0.30	0.20 ± 0.04	1.10 ± 0.29
Fe(3)	0.08 ± 0.01	< 0.040	< 0.032	0.7 ± 0.2	0.27 ± 0.05	0.64 ± 0.30
Fe(4)	0.09 ± 0.01	< 0.036	< 0.032	0.5 ± 0.2	0.30 ± 0.05	< 0.61
Pb(1)	0.06 ± 0.01	< 0.037	< 0.055	< 0.50	< 0.14	0.62 ± 0.27
Pb(2)	0.05 ± 0.01	< 0.034	< 0.053	< 0.40	< 0.13	0.78 ± 0.26
Pb(3)	0.13 ± 0.01	< 0.034	< 0.039	< 0.50	< 0.14	< 0.51
Pb(4)	0.11 ± 0.01	< 0.037	< 0.040	0.5 ± 0.2	< 0.15	0.63 ± 0.26

nent radiation damage at room temperature, while most of the dopants used do not cause permanent damage.

After an 18 Gy dose, the light yield of the doped crystals was measured again, as a function of the time after irradiation. The measurements were carried out under the exact same conditions as those used for the pre-irradiation measurements. The pulse heights of both doped and undoped samples were found to be reduced by 30 to 70% just after irradiation. The light output then increased with time, at (a stable) room temperature. The pulse heights measured as a function of time (Ph(t)) were then normalized to the pulse height observed prior to the irradiation (Ph_0) for each crystal.

Fig. 1 shows the normalized pulse height as a function of time after irradiation for some samples. The error bars shown in the figure are obtained by adding in quadrature the statistical and systematic errors.

It is obvious from fig. 1, that the recovery process can be described by a sum of at least two processes having different rates. This was observed for crystals doped with chemically dissimilar elements. The data also indicate that there might be another recovery process with a very short time constant as reported by Bobbink et al. in their early work [6]. We were, however, unable to resolve this short time constant from our

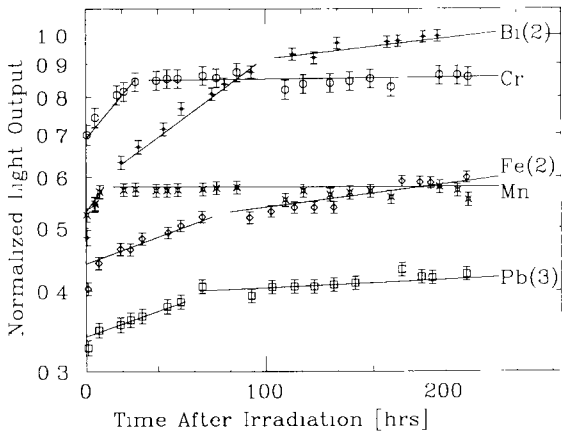

Fig. 1. The post-irradiation light output vs time, in log scale.

data. We then parametrized the normalized pulse height as a function of time:

$$\mathrm{Ph}(t)/\mathrm{Ph}_0 = 1 - a_1\, e^{-t/\tau_1} - a_2\, e^{-t/\tau_2}. \quad (1)$$

The results of the parametrization are shown in fig. 2. The time constants, τ_1, and τ_2, are listed in table 3.

From fig. 2 and table 3, we conclude that the dopant elements can be divided into three groups. Group I

Table 3
The light output and recovery after irradiation

Sample	PH_0 [channel]	τ_1 [h]	τ_2 [h]	Time after irradiation [h]			
				5	20	100	300
L(3)	169	13	174	0.69	0.75	0.87	0.90
HS	145	44	571	0.72	0.74	0.86	0.89
Bi(1)	157	82	520	0.53	0.60	0.82	0.95
Bi(2)	155	78	490	0.54	0.63	0.89	1.00
Ge(1)	173	25	540	0.46	0.48	0.57	0.66
Ge(2)	171	20	340	0.57	0.61	0.75	0.80
Al	160	6	120	0.54	0.60	0.82	0.98
Ca	162	62	580	0.57	0.63	0.83	0.93
Cu	158	47	570	0.51	0.59	0.81	0.88
Si	154	70	640	0.52	0.60	0.91	0.93
Co	154	50	470	0.44	0.49	0.63	0.70
Ga	160	15	450	0.48	0.52	0.66	0.72
Mg	166	18	460	0.51	0.54	0.67	0.78
Ni	150	16	640	0.50	0.53	0.62	0.68
Cr	86	14	3100	0.74	0.84	0.84	0.84
Mn	136	7	11500	0.55	0.56	0.57	0.57
Fe(1)	172	15	610	0.49	0.51	0.59	0.66
Fe(2)	156	18	880	0.44	0.46	0.54	0.60
Fe(3)	157	12	740	0.41	0.43	0.50	0.57
Fe(4)	–	–	–	0.44	0.49	0.55	0.63
Pb(1)	172	11	2800	0.41	0.43	0.46	0.46
Pb(2)	157	37	9054	0.38	0.40	0.45	0.45
Pb(3)	150	57	5954	0.35	0.36	0.40	0.43
Pb(4)	–	–	–	0.36	0.37	0.41	0.44

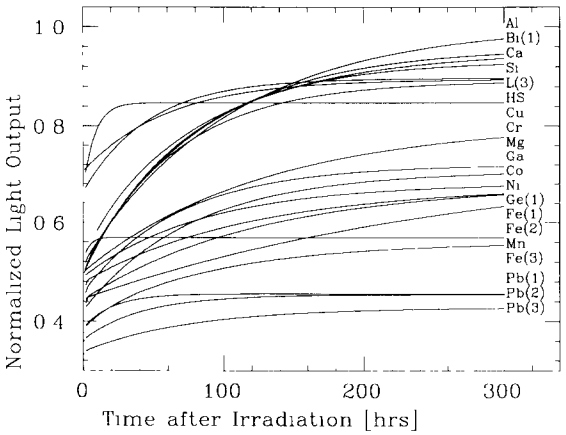

Fig 2 The post-irradiation normalized light output vs time.

contains those dopants that are very harmful and cause permanent or severe radiation damage: Cr, Mn, Fe, and Pb. In Group II we have those elements that are also harmful, but cause mild radiation damage: Co, Ga, Mg, and Ni. Group III contains elements that can be treated as harmless: Al, Ca, Cu, and Si. The presence of Group III elements in a crystal cannot be directly correlated with the damage, from our data.

The data also show that the rate of recovery from the initial damage is a function of the dopant. The extremely long recovery time constants of crystals doped with Cr, Mn, and Pb (more than 1000 hours) indicate that the radiation damage in these crystals is almost permanent at room temperature. While for other crystals, the recovery of radiation damage can be described by a sum of at least two exponentials, with the short time constant of an order of several ten hours and the long time constant of an order of several hundred hours. This result is consistent, quantitatively, with earlier measurements [5,6] obtained with undoped BGO crystals.

We also observed that the crystals produced with a stoichiometric excess of Bi in the melt show less damage and a faster recovery than those produced with an excess of Ge. Although we did not determine the stoichiometric purity of the final crystals, these data hint at the fact that the damage color center is related to deficiencies at bismuth-ion sites in a BGO crystal.

3.2. Absorption spectrum

The solid curves in fig. 3 show the absorption spectra measured before irradiation for four BGO crystals: BGO : Ca, BGO : Mn, BGO : Pb and BGO : Cr. We note that all the samples have the same absorption edge (306 nm). This indicates that the forbidden band width which is characteristic of BGO crystal (4.04 eV) is not changed by the impurity in the crystal.

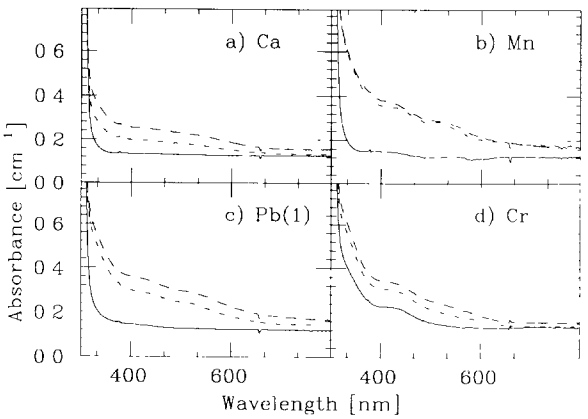

Fig. 3. The absorption spectra of some doped BGO crystals.

All samples have a small absorbence over the entire visible region of the spectrum. The only exception is the crystal doped with Cr. This crystal has strong absorption in the short wavelength region and thus appears yellowish. From fig. 3d, it is apparent that there are two absorption bands in the BGO sample doped with Cr: one is at 420 nm and the another is near 350 nm, which causes a shoulder close to the absorption edge.

By using a CARY 17 spectrophotometer, which has a higher resolution in the near-infrared region, an additional absorption peak was found around 750 nm. Fig. 4 shows the absorption spectra in a wavelength range between 300 and 1400 nm for the BGO sample doped with Cr. We attribute these three absorption bands to direct absorption by Cr^{3+} ions in the BGO [7].

3.2.1. Radiation-induced absorption bands

After a dose of 88 Gy, the absorption spectra were measured again as a function of time for each sample. The radiation-induced absorption was observed immediately after irradiation. The difference in the degree of darkening from sample to sample was also evident. The BGO sample doped with Mn, for example, appeared pinkish immediately after the irradiation.

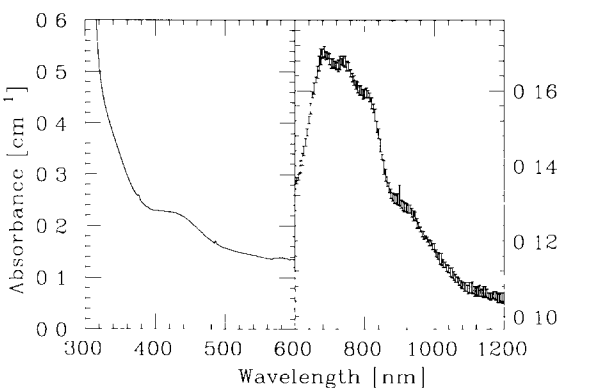

Fig. 4. The absorption due to the presence of Cr in BGO.

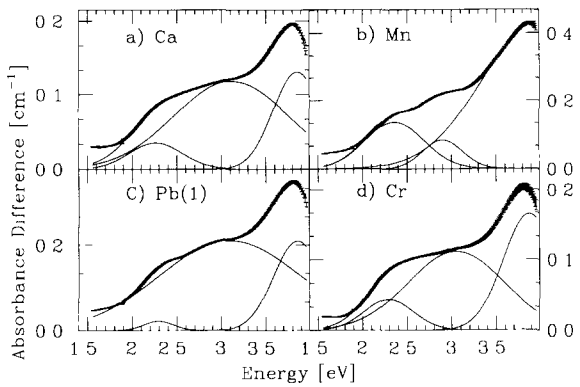

Fig 5. Gaussian decomposition of radiation-induced absorption in BGO.

Fig. 3 also shows the absorption spectra obtained at 5 min (dashed lines) and 20 h (dash-dotted lines) after the irradiation for four samples. A radiatior-induced absorption in BGO crystals is clearly seen in the figure. The data, however, show that the absorption edge of all samples (306 nm) was not changed by the irradiation. This indicates that the forbidden band width of BGO crystals (4.04 eV) is not changed by the irradiation.

In order to study the radiation-induced absorption, each spectrum obtained prior to irradiation was subtracted from the corresponding one measured 20 h after the irradiation. We found that the resultant radiation induced absorption can be decomposed into three broad absorption bands for all samples. Since the absorption bands are expected to have a Gaussian profile when expressed as a function of the photon energy, we then performed a least squares fit of the absorption spectra to the sum of three Gaussians:

$$\Delta A(E) = A_1 \, e^{-(E-E_1)^2/2\sigma_1^2} + A_2 \, e^{-(E-E_2)^2/2\sigma_2^2} + A_3 \, e^{-(E-E_3)^2/2\sigma_3^2}. \quad (2)$$

Fig. 5 shows the results of the fit for the same four BGO samples. The data are represented by a thick band in the plots, where the thickness of this band reflects the error in the measured spectra. The fit region was restricted to the energy range of 2.1 to 4.0 eV. It was found that the fitted peak positions are not sensitive to variations in the region of the spectrum used in the fit. The small systematic errors that we assign to the peak positions, however, are dominated by the choice of the region which is fitted. Table 4 lists the result of the fit for all BGO samples. The error bars shown in this table are the result of adding the statistical and systematic errors in quadrature.

A close look to the table reveals that these three radiation-induced absorption bands occur at the same energy, regardless of the dopant in the crystal. The

Table 4
The radiation-induced absorption bands in crystals

Sample	Fitted peak positions [eV]		
	E_1	E_2	E_3
L(3)	2.42 ± 0.08	3.00 ± 0.02	3.88 ± 0.05
HS	2.31 ± 0.01	3.07 ± 0.02	3.80 ± 0.04
Ge(1)	2.29 ± 0.01	3.00 ± 0.04	3.84 ± 0.04
Ge(2)	2.29 ± 0.01	3.00 ± 0.04	3.86 ± 0.04
Bi(1)	2.28 ± 0.01	3.00 ± 0.04	3.85 ± 0.05
Bi(2)	2.28 ± 0.01	2.98 ± 0.04	3.85 ± 0.05
Al	2.28 ± 0.02	3.03 ± 0.02	3.85 ± 0.02
Ca	2.27 ± 0.01	3.12 ± 0.02	3.84 ± 0.01
Cu	2.28 ± 0.02	2.99 ± 0.01	3.85 ± 0.02
Si	2.24 ± 0.05	3.02 ± 0.03	3.88 ± 0.06
Co	2.16 ± 0.01	3.00 ± 0.01	3.89 ± 0.01
Ga	2.22 ± 0.02	2.93 ± 0.01	3.89 ± 0.01
Mg	2.31 ± 0.02	2.96 ± 0.01	3.86 ± 0.02
Ni	2.28 ± 0.02	2.99 ± 0.02	3.86 ± 0.02
Cr	2.29 ± 0.01	3.01 ± 0.05	3.87 ± 0.01
Mn	2.38 ± 0.02	2.91 ± 0.01	3.99 ± 0.04
Fe(1)	2.29 ± 0.01	2.89 ± 0.08	3.84 ± 0.01
Fe(2)	2.35 ± 0.04	2.88 ± 0.08	3.98 ± 0.10
Fe(3)	2.35 ± 0.05	2.88 ± 0.03	3.76 ± 0.24
Fe(4)	2.34 ± 0.05	2.97 ± 0.08	3.77 ± 0.24
Pb(1)	2.30 ± 0.01	3.05 ± 0.06	3.84 ± 0.03
Pb(2)	2.35 ± 0.03	2.91 ± 0.06	3.93 ± 0.40
Pb(3)	2.35 ± 0.04	3.15 ± 0.06	3.84 ± 0.03
Pb(4)	2.28 ± 0.04	2.97 ± 0.04	3.92 ± 0.08

energies of these bands can be summarized as 2.3 ± 0.1, 3.0 ± 0.1, and 3.8 ± 0.1 eV.

As a systematic check, we also measured the radiation-induced absorption bands of a Harshaw BGO crystal (HS) and a sample of rock salt. The energies of three bands observed in the Harshaw crystal, 2.31 ± 0.01, 3.07 ± 0.02, and 3.80 ± 0.04, indicate that the observed three bands do not originate from some common impurities existing in BGO crystals from SIC. Only one radiation-induced absorption band was observed in the rock salt sample. The measured energy and FWHM are 2.69 and 0.48 eV, respectively. These values are consistent with the well-known radiation induced F-center (halogen vacancy a with a trapped electron) which has an energy and FWHM of 2.66 and 0.47 eV, respectively. This confirms that our energy determination is accurate to within 1%.

The observation of these three common absorption bands in the BGO hints at the fact that the impurity in the crystal acts only as a "catalytic agent", which activates pre-exisiting color centers to produce the radiation damage effect. The nature of the color center is not a function of impurity type, rather of the crystals itself, e.g., of Bi and/or Ge. This makes it unlikely that the detection and elimination of just one or a few

impurities in the manufacturing process will make the crystal highly radiation resistant.

3.2.2. Infrared absorption spectrum

In order to investigate any radiation damage effect due to a metamict crystal we measured the infrared absorption spectra of some samples. The data show no deviation in the absorption spectra for doped versus undoped BGO crystals. There were also no differences observed between the absorption spectra before and after irradiation. This indicates that the damage color center occurs at the level of the trapping sites caused by the presence of impurities, rather than being caused by disruption of the crystal lattice. The absence of any infrared absorption peaks also hints that neither molecular water or OH^- radicals play a role in the radiation chemistry of the BGO [8].

3.3. High-temperature curing of radiation damage

As discussed in section 3.1, the radiation damage in BGO crystals recovers slowly at the room temperature, with a typical long time constant of the order of a few hundred hours. The crystals doped with Cr, Mn and Pb, however, almost never recover at room temperature: their recovery times are well in excess of 1000 h. By heating the crystal to 200°C for a few tens of minutes, all the samples were found to have recovered completely. This observation is in agreement with earlier reports from other groups [5,6].

The recovery is associated with an emission of light (thermoluminescence), which has been studied by several groups [9]. We note that when a Mn doped sample was heated to 200°C a "*glow peak*" was observed in the thermoluminescence data for this crystal [10].

4. Conclusions

We summarize our main observations in this report as follows:

- Trace impurities of Cr in a BGO crystal causes permanent damage, which substantially decrease the light output of crystals. Three absorption peaks from Cr^{3+} were observed in Cr doped BGO.
- The rate of recovery from the initial radiation damage is a function of the dopant. The recovery process can be described by a sum of at least two exponentials. For most crystals the short time constant is in the order of several tens of hours, and the long time constant is in the order of several hundred hours. For crystals doped with Cr, Mn, and Pb, the longer time constants exceed 1000 hours, indicating that the radiation damage in these crystals is (nearly) permanent at room temperature.
- The degree to which a BGO crystal is susceptible to radiation damage is also a function of the chemical nature of the impurity. Crystals doped with Cr, Mn, Fe, and Pb show a severe radiation damage effect, while crystals doped with Co, Ga, Mg, and Ni show a moderate radiation damage effect. Crystals doped with Al, Ca, Cu, and Si show only a minimal effect.
- BGO containing a stoichiometric excess of Bi is less damaged by radiation and recovers faster than BGO that has an excess of Ge.
- The radiation damage of BGO crystals can be cured by heating the crystals to 200°C for several tens of minutes.
- The radiation-induced absorption spectra of BGO can be decomposed into three broad absorption bands. The bands occur at the same positions in all doped and undoped crystals: 2.3 ± 0.1, 3.0 ± 0.11, and 3.8 ± 0.1 eV.
- The damage color centers in BGO occur, not at the site of impurity elements, but rather at either the Bi and/or Ge and/or O site. The impurities play a role of an agent, probably by providing free electrons or holes, so that color centers which trap electrons or holes can be "activated" at one of the possible sites mentioned above.

Acknowledgements

We would like to thank Prof. G. Rossman of Caltech for many useful discussions, and for the use of spectrophotometric lab facilities. Prof. R. Gomez of Caltech provided the electronics to perform the pulse height analysis. We are grateful to Mr. J.Y. Lian, Q.S. Shen, B.F. Shen and P.F. Shao at SIC for their help in the preparation of the samples used in this work.

References

[1] M.J. Webber and R.R. Monchamp, J. Appl. Phys 44 (1973) 5496.
[2] L3 Collaboration, L3 Technical Proposal, May 1983; J. Bakken et al., Nucl. Instr. and Meth A254 (1987) 536 and A228 (1985) 294.
[3] M. Kobayashi et al., Nucl. Instr and Meth. A200 (1983) 107
[4] T.Q Zhou et al., Nucl. Instr. and Meth A258 (1987) 464.
[5] C. Laviron and P. Lecoq, Nucl. Instr. and Meth. A227 (1984) 75.
[6] G.J. Bobbink et al., Nucl. Instr. and Meth. A227 (1984) 470.
[7] C.P. Poole, J. Phys. Chem. Solids 25 (1964) 1169.
[8] R.D. Aines and G. Rossman, Am Mineral. 71 (1986) 1169.
[9] B. Esser, Luminescence Under Radiattion Damage and Thermoluminescence of Bismuth Germanate, ISSN-0174-500X RWTH (Aachen, 1984).
[10] R. Melcher, private communication.